Progress In Electromagnetics Research, PIER 54, 1–17, 2005

EDGE-PRESERVING REGULARIZATION SCHEME APPLIED TO THE MODIFIED GRADIENT METHOD FOR THE RECONSTRUCTION OF TWO-DIMENSIONAL TARGETS FROM LABORATORY-CONTROLLED DATA

K. Belkebir

Institut Fresnel, UMR-CNRS 6133
Campus de Saint Jérôme, case 162
13397 Marseille Cedex 20, France

A. Baussard †

L2S, UMR-CNRS 8506
3 rue Joliot-Curie, 91192 Gif-sur-Yvette, France

D. Prémel ‡

SATIE, UMR-CNRS 8029
61 avenue du Président Wilson
94235 Cachan Cedex, France

Abstract—In this paper, a two-dimensional inverse scattering problem dealing with microwave tomography is considered. To solve this non linear and ill-posed problem, an iterative scheme based on the Modified Gradient Method (MGM) is used. The object to be estimated is represented by a complex function, and some modifications of the MGM formulation have been considered. This algorithm leads to an efficient regularization scheme, based on edge preserving functions which act separately on the real and imaginary parts of the object. In order to show the interest of this regularized MGM, the algorithm is tested against laboratory-controlled microwave data.

† He is now with E3I2 - ENSIETA, 2 rue François Verny, 29806 Brest, France
‡ Also with CEA Saclay, DRT/DETECS/SYSSC/LCME, 91191 Gif-sur-Yvette, France.

1. INTRODUCTION

Various inverse scattering problems use electromagnetic waves. They aim at determining the location and the spatial variations of some physical properties inside a test area. For instance, in microwave imaging, the goal is to reconstruct the complex permittivity distribution of an object (the real part representing the permittivity and the imaginary part the conductivity). Several algorithms have been developed to solve this non linear and ill-posed problem. In this contribution, an iterative scheme based on the modified gradient method introduced by Kleinman and Van den Berg [9] is considered. It consists of updating simultaneously, at each iteration, the unknown field in the scattering domain and the unknown material contrast by minimizing a cost functional composed of two normalized terms.

In this paper, in order to take into account that the object to be estimated is represented by a complex function, some modifications of the MGM formulation have been made [2]. Moreover, to improve the quality of the reconstructions, a regularization term, which introduces *a priori* knowledge, is added. In [13], an additive Total Variation (TV) regularization procedure was incorporated in the initial modified gradient method. The reported results clearly display significant improvements in the reconstruction. Different regularization schemes can be considered; in this paper the authors investigate an edge-preserving approach [6]. This regularizing method has already shown its usefulness for image enhancement [6] and image reconstruction

[11, 8] using a conjugate gradient algorithm. As far as the authors know, this regularization approach has not been applied to the Modified Gradient Method (MGM) nor validated against experimental data.

Taking advantage of the considered MGM formulation, two regularization functions acting separately on the real and imaginary parts of the object are considered. Moreover, taking into account [7], the edge-preserving regularization scheme is directly implemented without considering a half-quadratic technique as previously done [5, 6, 8, 11]. To test this regularized MGM and to show the potentialities of this approach, the algorithm is tested against some laboratory-controlled microwave data.

The paper is organized as follows: in Section 2, the statement of the problem is presented. In Section 3, the formulation of the MGM algorithm is presented. Section 4 presents the regularized MGM scheme, considering an edge-preserving regularization term. Section 5 shows results of reconstruction of dielectric and metal targets from real data. Finally, Section 6 gives some concluding remarks.

2. FORMULATION OF THE PROBLEM

The geometry of the problem studied in this paper is shown in Figure 1 where a two-dimensional object of arbitrary cross-section Ω_0 is confined in a bounded domain Ω. The embedding medium Ω_b is assumed to be infinite and homogeneous, with permittivity $\varepsilon_b = \varepsilon_0\varepsilon_{br}$, and of permeability $\mu = \mu_0$ (ε_0 and μ_0 being the permittivity and permeability of the vacuum, respectively). The scatterers are assumed to be inhomogeneous cylinders with complex permittivity distribution $\varepsilon(\mathbf{r}) = \varepsilon_0\varepsilon_r(\mathbf{r})$; the entire configuration is non-magnetic ($\mu = \mu_0$).

A right-handed Cartesian coordinate frame (O, $\mathbf{u}_x$, $\mathbf{u}_y$, $\mathbf{u}_z$) is defined. The origin O can be either inside or outside the scatterer and the z-axis is parallel to the invariance axis of the scatterer. The position vector $\mathbf{OM}$ can then be written as

$$\mathbf{OM} = x\mathbf{u}_x + y\mathbf{u}_y + z\mathbf{u}_z = \mathbf{r} + z\mathbf{u}_z. \tag{1}$$

The sources that generate the electromagnetic excitation are assumed to be lines parallel to the z-axis, located at $(\mathbf{r}_l)_{1\leq l\leq L}$. Taking into account a time factor $\exp(-i\omega t)$, in the Transverse Magnetic (TM) case, the time-harmonic incident electric field created by the l^{th} line source is given by

$$\mathbf{E}_l^{\text{inc}}(\mathbf{r}) = E_l^{\text{inc}}(\mathbf{r})\mathbf{u}_z = P\frac{\omega\mu_0}{4}H_0^{(1)}(k_b|\mathbf{r} - \mathbf{r}_l|)\mathbf{u}_z, \tag{2}$$

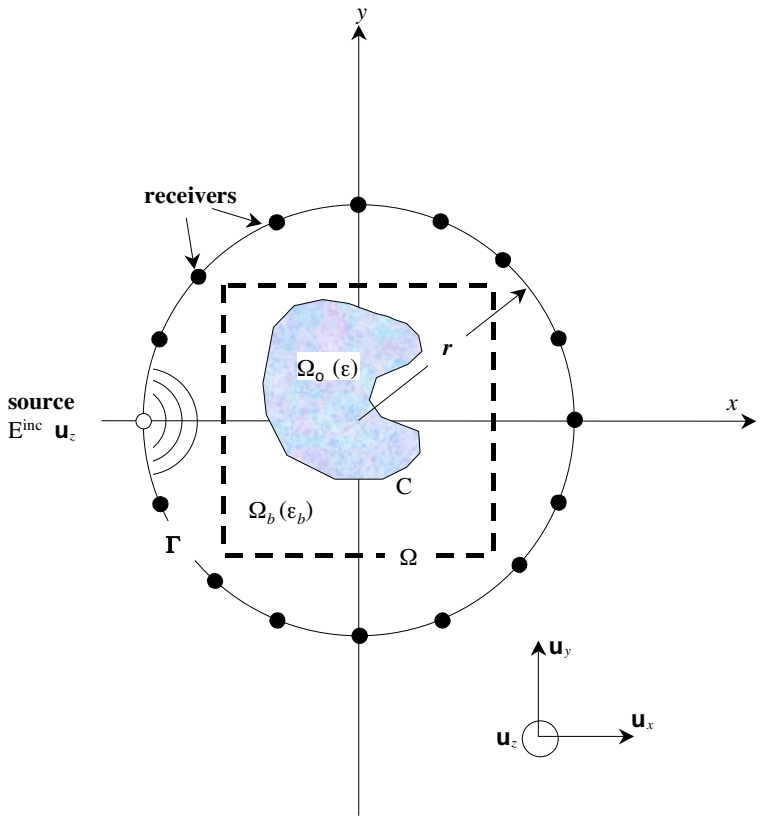

Figure 1. Geometry of the problem.

where P is the strength of the electric source, ω the angular frequency, $H_0^{(1)}$ the Hankel function of zero order and of the first kind and k_b the wavenumber in the surrounding medium.

For the inverse scattering problem we assume that the unknown object is successively illuminated by L electromagnetic excitations and for each incident field the scattered field is available along a contour Γ at M positions. For each excitation, the direct scattering problem may be reformulated as two coupled contrast-source integral relations: the observation equation (3) and the coupling equation (4)

$$E_l^{\mathrm{d}}(\mathbf{r} \in \Gamma) = k_0^2 \int_\Omega \chi(\mathbf{r}') E_l(\mathbf{r}') G(\mathbf{r}, \mathbf{r}') \mathrm{d}\mathbf{r}', \tag{3}$$

$$E_l(\mathbf{r} \in \Omega) = E_l^{\mathrm{inc}} + k_0^2 \int_\Omega \chi(\mathbf{r}') E_l(\mathbf{r}') G(\mathbf{r}, \mathbf{r}') \mathrm{d}\mathbf{r}', \tag{4}$$

where $\chi(\mathbf{r}) = \varepsilon_r(\mathbf{r}) - \varepsilon_{br}$ denotes the permittivity contrast which vanishes outside $\Omega \supset \Omega_0$, $G(\mathbf{r}, \mathbf{r}')$ is the two-dimensional homogeneous free space Green function and k_0 represents the wavenumber in the vacuum. For the sake of simplicity, the Equations (3) and (4) are rewritten in operator notation as

$$E_l^{\mathrm{d}} = \mathbf{G}_\Gamma \chi E_l, \tag{5}$$

$$E_l = E_l^{\mathrm{inc}} + \mathbf{G}_\Omega \chi E_l. \tag{6}$$

3. MODIFIED GRADIENT METHOD

The inverse scattering problem consists in finding the complex contrast function χ in the investigated area Ω from the measured scattered field, the total field E_l being also unknown. In order to solve this problem, a modified gradient method [9] is considered. This approach consists in constructing two sequences, related to the contrast $\{\chi_n\}$ and to the total field $\{E_{l,n}\}$, using the following recursive relations

$$\chi_n = \chi_{n-1} + \beta_n d_n, \tag{7}$$

$$E_{l,n} = E_{l,n-1} + \alpha_{l,n} v_{l,n}, \tag{8}$$

where d_n and $v_{l,n}$ are search directions with respect to χ_n and $E_{l,n}$, respectively. The scalar coefficients β_n and $\alpha_{l,n}$ are chosen at each iteration step n such that they minimize the normalized cost functional $F_n(\chi_n, E_{l,n})$ given by

$$F_n(\chi_n, E_{l,n}) = W_\Omega \sum_{l=1}^{L} \|h_{l,n}^{(1)}\|_\Omega^2 + W_\Gamma \sum_{l=1}^{L} \|h_{l,n}^{(2)}\|_\Gamma^2, \tag{9}$$

where W_Ω and W_Γ are the normalizing coefficients defined as

$$W_\Omega = \frac{1}{\sum_{l=1}^{L} \|E_l^{\mathrm{inc}}\|_\Omega^2}, \quad W_\Gamma = \frac{1}{\sum_{l=1}^{L} \|E_l^{\mathrm{d}}\|_\Gamma^2}. \tag{10}$$

The functions $h_{l,n}^{(1)}$ and $h_{l,n}^{(2)}$ are the residual errors in the field equation (6) and in the observation equation (5), respectively. They are defined as follows

$$h_{l,n}^{(1)} = E_l^{\mathrm{inc}} - E_{l,n-1} + \mathbf{G}_\Omega \chi_n E_{l,n}, \tag{11}$$

$$h_{l,n}^{(2)} = E_l^{d} + \mathbf{G}_\Gamma \chi_n E_{l,n}. \tag{12}$$

When dealing with the reconstruction of complex objects, it is recommended to consider separately the real and imaginary part

of the contrast function [8]. Therefore, in order to obtain an efficient implementation of the MGM, the complex contrast function is redefined as follows

$$\chi_n = \xi_n + i\eta_n - \varepsilon_{br}, \tag{13}$$

where ξ_n and η_n are two real auxiliary functions. Then, the recursive relations with respect to the complex function χ_n are defined as

$$\xi_n = \xi_{n-1} + \beta_n^{\xi} d_n^{\xi}, \tag{14}$$
$$\eta_n = \eta_{n-1} + \beta_n^{\eta} d_n^{\eta}, \tag{15}$$

where all quantities are real. The minimization of F_n is achieved by using the Polak-Ribière conjugate gradient method [12] where the search directions d_n^{ξ} and d_n^{η} are the standard Polak-Ribière conjugate gradient directions

$$d_n^{\xi} = g_n^{\xi} + \gamma_n^{\xi} d_{n-1}^{\xi} \text{ with } \gamma_n^{\xi} = \frac{\langle g_n^{\xi} | g_n^{\xi} - g_{n-1}^{\xi} \rangle_{\Omega}}{\| g_{n-1}^{\xi} \|_{\Omega}^2}, \tag{16}$$

$$d_n^{\eta} = g_n^{\eta} + \gamma_n^{\eta} d_{n-1}^{\eta} \text{ with } \gamma_n^{\eta} = \frac{\langle g_n^{\eta} | g_n^{\eta} - g_{n-1}^{\eta} \rangle_{\Omega}}{\| g_{n-1}^{\eta} \|_{\Omega}^2}, \tag{17}$$

where $< .|. >_D$ represents the inner product defined on $L^2(D)$ and g_n^{ξ} and g_n^{η} are the gradients of the cost functional $F_n(\xi_n, \eta_n, E_{l,n})$ with respect to ξ_n and η_n, respectively, evaluated at the $(n-1)$th step assuming that the total field inside the test domain does not change.

These gradients are given by

$$g_n^{\xi} = \Re e \left[W_{\Omega} \sum_{l=1}^{L} \bar{E}_{l,n-1} \mathbf{G}_{\Omega}^{\dagger} h_{l,n-1}^{(1)} - W_{\Gamma} \sum_{l=1}^{L} \bar{E}_{l,n-1} \mathbf{G}_{\Gamma}^{\dagger} h_{l,n-1}^{(2)} \right], \tag{18}$$

$$g_n^{\eta} = \Im m \left[W_{\Omega} \sum_{l=1}^{L} \bar{E}_{l,n-1} \mathbf{G}_{\Omega}^{\dagger} h_{l,n-1}^{(1)} - W_{\Gamma} \sum_{l=1}^{L} \bar{E}_{l,n-1} \mathbf{G}_{\Gamma}^{\dagger} h_{l,n-1}^{(2)} \right], \tag{19}$$

where $\bar{E}$ denotes the complex conjugate of the field E, while $\mathbf{G}_{\Omega}^{\dagger}$ and $\mathbf{G}_{\Gamma}^{\dagger}$ denote the adjoint operators of $\mathbf{G}_{\Omega}$ and $\mathbf{G}_{\Gamma}$, respectively.

The search direction for the total field is defined as

$$v_{l,n} = g_{l,n}^{v} + \gamma_{l,n}^{v} v_{l,n-1} \text{ with } \gamma_{l,n}^{v} = \frac{\langle g_{l,n}^{v} | g_{l,n}^{v} - g_{l,n-1}^{v} \rangle_{\Gamma}}{\| g_{l,n-1}^{n} \|_{\Gamma}^2}. \tag{20}$$

where $g_{l,n}^{v}$ is the gradient of the cost functional $F_n(\xi_n, \eta_n, E_{l,n})$ with respect to $E_{l,n}$, evaluated at the $(n-1)$ th step assuming that ξ_n and

η_n do not change. This gradient is given by

$$g_{l,n}^{v} = W_\Omega \left[\bar{\chi}_{n-1}\mathbf{G}_\Omega^\dagger h_{l,n-1}^{(1)} - h_{l,n-1}^{(1)}\right] - W_\Gamma \bar{\chi}_{n-1}\mathbf{G}_\Gamma^\dagger h_{l,n-1}^{(2)}. \tag{21}$$

4. DETERMINISTIC EDGE-PRESERVING REGULARIZATION

4.1. Regularized Modified Gradient Method

In order to improve the final reconstructions, a regularizing term which introduces *a priori* knowledge on the object to be reconstructed is added to the previous MGM scheme. Dealing with complex-valued contrasts, two regularizing terms, which separately act on the real and the imaginary parts of the contrast function, are introduced. In this way, the considered general cost functional $\tilde{F}_n(\xi_n, \eta_n, E_{l,n})$ can be defined as

$$\tilde{F}_n(\xi_n, \eta_n, E_{l,n}) = F_n(\xi_n, \eta_n, E_{l,n}) + F_n^\xi(\xi_n) + F_n^\eta(\eta_n), \tag{22}$$

where F_n^ξ and F_n^η are regularizing terms acting on the real and imaginary parts, respectively. Note that the regularization terms could be different.

With this formulation, the modification of the MGM algorithm is essentially noticeable on the contrast search directions. The recursive relations for the regularized MGM are then given by

$$\xi_n = \xi_{n-1} + \beta_n^\xi \tilde{d}_n^\xi, \tag{23}$$

$$\eta_n = \eta_{n-1} + \beta_n^\eta \tilde{d}_n^\eta, \tag{24}$$

$$E_{l,n} = E_{l,n-1} + \alpha_{l,n} v_{l,n}, \tag{25}$$

where $\tilde{d}_n^\xi$ and $\tilde{d}_n^\eta$ are the search directions with respect to ξ_n and η_n, respectively. These regularized updating directions are defined as follows

$$\tilde{d}_n^\xi = \tilde{g}_n^\xi + \tilde{\gamma}_n^\xi \tilde{d}_{n-1}^\xi \qquad \text{with} \qquad \tilde{\gamma}_n^\xi = \frac{\langle \tilde{g}_n^\xi | \tilde{g}_n^\xi - \tilde{g}_{n-1}^\xi \rangle_\Omega}{\|\tilde{g}_{n-1}^\xi\|_\Omega^2}, \tag{26}$$

$$\tilde{d}_n^\eta = \tilde{g}_n^\eta + \tilde{\gamma}_n^\eta \tilde{d}_{n-1}^\eta \qquad \text{with} \qquad \tilde{\gamma}_n^\eta = \frac{\langle \tilde{g}_n^\eta | \tilde{g}_n^\eta - \tilde{g}_{n-1}^\eta \rangle_\Omega}{\|\tilde{g}_{n-1}^\eta\|_\Omega^2}, \tag{27}$$

where $\tilde{g}_n^\xi$ and $\tilde{g}_n^\xi$ are the gradients of the cost functional $\tilde{F}_n(\xi_n, \eta_n, E_{l,n})$ with respect to ξ_n and η_n, respectively. In fact, it can be easily shown

that the search directions $\tilde{d}_n^{\xi}$ and $\tilde{d}_n^{\eta}$ correspond to

$$\tilde{d}_n^{\xi} = d_n^{\xi} + \hat{d}_n^{\xi}, \tag{28}$$

$$\tilde{d}_n^{\eta} = d_n^{\eta} + \hat{d}_n^{\eta}, \tag{29}$$

where $\hat{d}_n^{\xi}$ and $\hat{d}_n^{\eta}$ are the regularizing search directions which depend on the choice of the regularization terms.

4.2. Edge-Preserving Regularization

In this contribution, an edge-preserving regularization approach [6] is considered. The regularization term is defined as follows

$$F^{EP}(t) = \rho \int_{\Omega} \varphi\left(\|\nabla t(\mathbf{r})\|\right) \mathrm{d}\mathbf{r}, \tag{30}$$

where φ is a regularization function which smoothes the homogeneous area isotropically while preserving edges, and ρ is the weighting parameter which fixes the influence of the regularization term. Different conditions have been defined in order to ensure edge preservation [5, 6]. These conditions are based on the study of the derivative of (30), formally given by

$$-\nabla\left(\frac{\varphi\left(\|\nabla t(\mathbf{r})\|\right)}{\|\nabla t(\mathbf{r})\|}\nabla t(\mathbf{r})\right). \tag{31}$$

The three main assumptions for the function $\frac{\varphi'(t)}{t}$ are

- $\lim\limits_{t\to 0} \dfrac{\varphi'(t)}{t} = M < \infty$ isotropic smoothing in the homogeneous area.
- $\lim\limits_{t\to \infty} \dfrac{\varphi'(t)}{t} = 0$: edge preserving.
- $\dfrac{\varphi'(t)}{t}$ strictly decreasing.

In Table 1, four main functions are reviewed. The choice of the function used in a given reconstruction depends on the object to be estimated.

If we consider the discretized search domain as an image of dimension N_{lig} and N_{col} indexed by *lig* (row number) and *col* (column number), the regularizing term can be written as follows

$$F^{EP}(t) = \sum_{lig=1}^{N_{lig}} \sum_{col=1}^{N_{col}} \rho\varphi\left(\frac{\|\nabla t(\mathbf{r})\|}{\delta}\right), \tag{32}$$

Table 1. Edge-preserving functions.

function φ	$\varphi(t)$	$\frac{\varphi'(t)}{t}$
Geman and Mc.Clure	$\frac{t^2}{1+t^2}$	$\frac{2}{(1+t^2)^2}$
Hebert and Leahy	$\log(1+t^2)$	$\frac{2}{1+t^2}$
Hyper surfaces	$\sqrt{1+t^2}+1$	$\frac{1}{\sqrt{1+t^2}}$
Green	$\log[\cosh(t)]$	$\begin{cases} 1 & t=0 \\ \frac{\tanh(t)}{t} & t=0 \end{cases}$

where δ fixes the threshold discontinuity level on the gradient norm.

Previously, this regularizing term was implemented within an half-quadratic technic [5, 11, 8]. Here, according to [7], we do not consider this approach but directly implement our cost functional as

$$\tilde{F}_n(\xi_n, \eta_n, E_{l,n}) = F_n(\xi_n, \eta_n, E_{l,n}) + F_n^{\xi}(\xi_n) + F_n^{\eta}(\eta_n), \tag{33}$$

where

$$F_n^{\xi}(\xi_n) = \sum_{lig=1}^{N_{lig}} \sum_{col=1}^{N_{col}} \rho_{\xi} \varphi \left(\frac{\|\nabla \xi_n(\mathbf{r})\|}{\delta_{\xi}} \right), \tag{34}$$

$$F_n^{\eta}(\eta_n) = \sum_{lig=1}^{N_{lig}} \sum_{col=1}^{N_{col}} \rho_{\eta} \varphi \left(\frac{\|\nabla \eta_n(\mathbf{r})\|}{\delta_{\eta}} \right), \tag{35}$$

$(\rho_{\xi}, \delta_{\xi})$ and $(\rho_{\eta}, \delta_{\eta})$ are the parameters applied for the real and imaginary parts, respectively.

For the images, the following computational relations were considered

$$(\nabla_x t)_{(lig,col)} = t(lig+1, col) - t(lig, col), \tag{36}$$

$$(\nabla_y t)_{(lig,col)} = t(lig, col+1) - t(lig, col), \tag{37}$$

$$\|\nabla t\|^2_{(lig,col)} = \|\nabla_x t\|^2_{(lig,col)} + \|\nabla_y t\|^2_{(lig,col)}. \tag{38}$$

It is noteworthy that without a contrast function defined as (13) and a regularization scheme which acts separately on the real and imaginary parts of the object, the real and imaginary parameters (ρ_ξ, δ_ξ) and (ρ_η, δ_η) would affect both object parts, making their choice difficult and finally impossible.

Moreover, since an initial estimate must be used to initialize the MGM algorithm, the back-propagation method from [3] was considered. Furthermore, considering [10], when the variation of two successive criterion values do not vary within a given range (about 10^{-6}), the total field is fully computed using Equation (6). The process is stopped if the criterion value between two iterations does not change or if the maximum number of iterations, fixed at the beginning of the process, is reached. The number of iterations depends on the complexity (shape, permittivity level, etc.) of the estimated object.

5. NUMERICAL RESULTS

5.1. Experimental Setup

The experimental setup (Figure 2) under consideration, from Institut Fresnel (Marseille, France), is described in [3, 4]. A dielectric or metallic homogeneous object is irradiated by $L = 36$ different locations

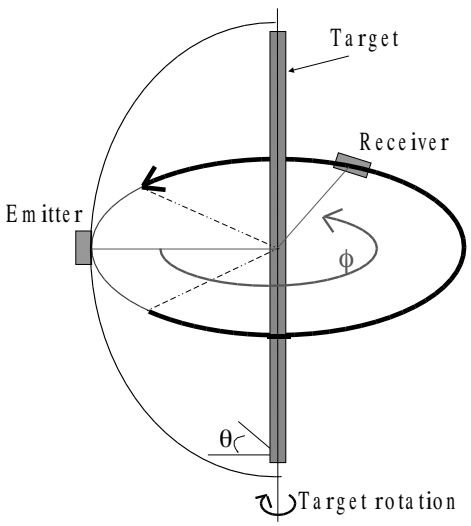

Figure 2. The experimental setup geometry used for validating the inverse algorithm. ϕ denotes the angle of receiving antenna while θ represents the angle of the emitting antenna.

evenly distributed around the object. The TM polarized incident field, $E_l^{\text{inc}}\,(l = 1, \cdots, L)$, is modelled in the investigation domain by a linearly polarized isotropic cylindrical wave as defined in (2). The scattered field for each irradiation E_l^{d} is measured for $M = 72$ different locations evenly distributed around the object. However, due to physical limitations, there is a blind zone of 60°, from each part of the transmitter, such that the scattered field is measured for 49 out of the 72 receiver angles.

In what follows, some reconstructions using the experimental data are presented.

5.2. Two Dielectric Objects

A dielectric target made of twin cylinders with circular cross-section of radius 1.5 cm is considered. The relative permittivity of this target was estimated to be $\varepsilon_r = 3 \pm 0.3$. In this contribution, we report reconstructions obtained at the operating frequencies of 4 GHz and 7 GHz (see [4] for more details on the experimental setup, in which the target under test is referred therein as **TwodielTM_8f**). In both cases, a rectangular search domain of 8 cm (along the x-axis) $\times$16 cm (along the y-axis), discretized into 20×40 cells and centered at ($x = 0$ cm, $y = 0$ cm) was considered.

Figures 3 and 4 show the discretized simulated search domain, the

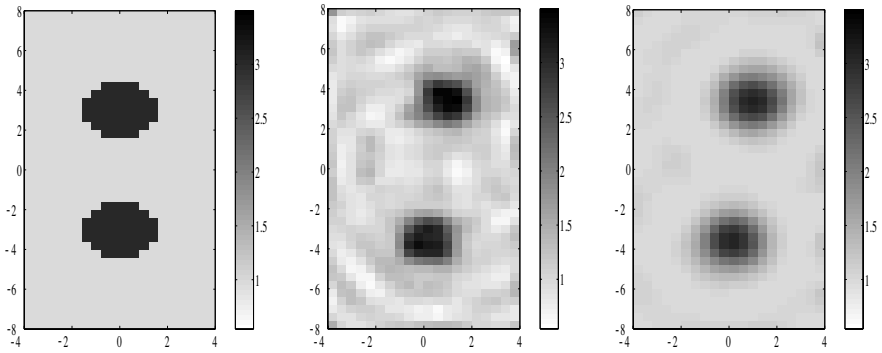

(a) (b) (c)

Figure 3. Reconstructions obtained after 150 iterations of the two dielectric objects at 4 GHz. (a) Simulated 8 cm $\times$ 16 cm search domain centered at ($x = 0$ cm, $y = 0$ cm) and discretized into 20×40 cells. (b) Reconstruction obtained without regularization. (c) Reconstruction obtained with regularization.

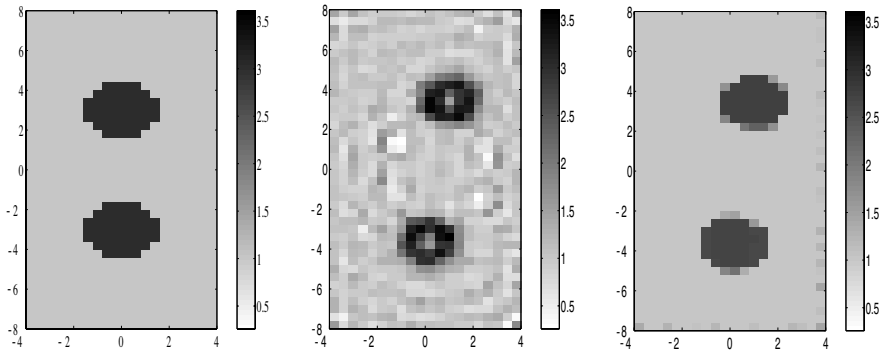

(a) (b) (c)

Figure 4. Reconstructions obtained after 150 iterations of the two dielectric objects at 7 GHz. (a) Simulated 8 cm × 16 cm search domain centered at ($x = 0$ cm, $y = 0$ cm) and discretized into 20×40 cells. (b) Reconstruction obtained without regularization. (c) Reconstruction with regularization.

reconstructions obtained without regularization and the reconstructions using the edge-preserving regularization (with a Geman and Mc Clure function φ). The reconstructed imaginary part of the contrast was found almost homogeneous and of small magnitude. Therefore, we conclude that the object under test is dielectric.

The permittivity level at 4 GHz is $\varepsilon_r = 3.49$ and $\varepsilon_r = 3.56$ at 7 GHz in the non regularized case and $\varepsilon_r = 3.11$ at 4 GHz and $\varepsilon_r = 2.77$ at 7 GHz in the regularized one. These results show the improvement of the reconstruction — for the shape and the permittivity level — when using the regularized MGM. In the obtained results a shift of the cylinders can be notice. This shift is due to experimental positioning errors (which are within the experimental margin).

5.3. Rectangular Metallic Object

The metallic target is a centered cylinder with a rectangular cross-section of $(1.27 \times 2.54)\,\text{cm}^2$. The experimental data are fully described in [4] and the target is referred therein as **rectTM_cent**. For frequencies of 8 GHz and 16 GHZ, a 2.1 cm × 3.2 cm search domain, discretized into 20×30 cells and centered at ($x = -0.5$ cm, $y = -0.75$ cm) was considered.

Figures 5 and 6 show the simulated search domain, the reconstructions obtained after 50 iterations without regularization and using the regularized MGM (with a Hebert and Leahy function φ).

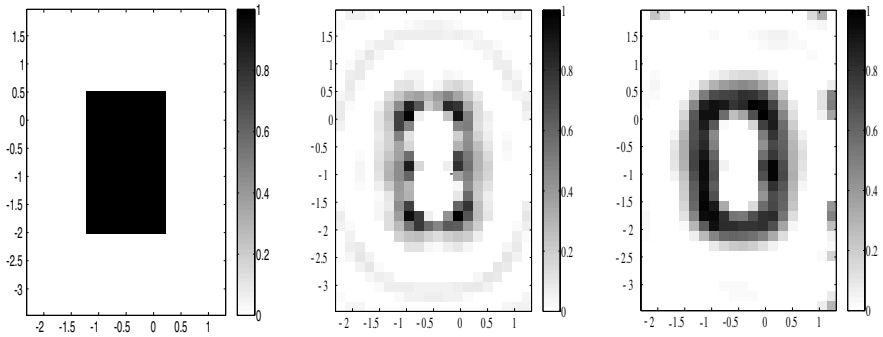

(a) (b) (c)

Figure 5. Reconstructions of the metallic target at 8 GHz after 100 iterations. Grey scale level of the (a) Simulated $3.6 \times 5.4\,\mathrm{cm}^2$ search domain centered at ($x = -0.5\,\mathrm{cm}$, $y = -0.75\,\mathrm{cm}$) and discretized into 20×30 cells, (b) reconstructed target without regularization and (c) reconstruction obtained using the regularized MGM.

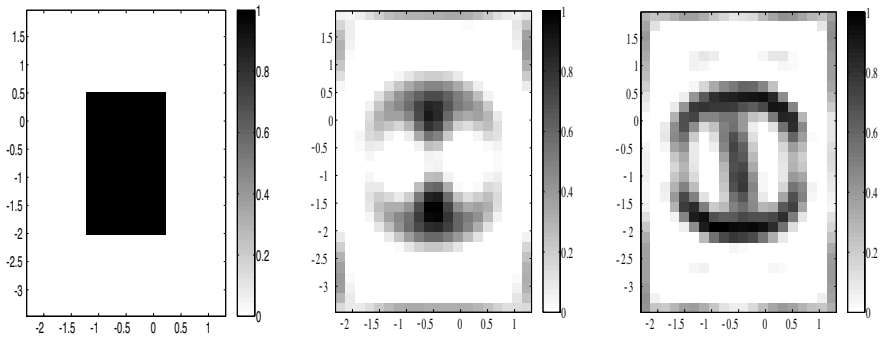

(a) (b) (c)

Figure 6. Reconstructions of the metallic target at 16 GHz after 100 iterations. Grey scale level of the (a) Simulated $3.6 \times 5.4\,\mathrm{cm}^2$ search domain centered at ($x = -0.5\,\mathrm{cm}$, $y = -0.75\,\mathrm{cm}$) and discretized into 20×30 cells, (b) reconstructed target without regularization and (c) reconstruction obtained using the regularized MGM.

These figures present only the grey-level map of the normalized non negative reconstructions, since for such impenetrable objects only the shape is of interest; the estimated conductivity level is less important. The real part of the contrast was found more or less homogeneous inside the search domain and close to unity. Therefore, they are not presented.

Maximum conductivity at 8 GHz is $\sigma = 3.45\,\mathrm{S/m}$ and $\sigma = 3.31\,\mathrm{S/m}$ at 16 GHz in the non regularized case. In the regularized case, the maximum estimated conductivity at 8 GHz is $\sigma = 1.50\,\mathrm{S/m}$ and $\sigma = 0.29\,\mathrm{S/m}$ at 16 GHz. Let us notice that the reconstruction obtained at 8 GHz seems to correspond to an 'equivalent' object.

5.4. "U-Shaped" Metallic Object

In this part, a "U-shaped" metallic cylinder defined within a $(8\times5)\,\mathrm{cm}^2$ rectangle is considered. The shape of the target under test is described in [4] and referred therein as **uTM_shaped** for which data were carried out with 8 frequencies ranging from 2 up to 16 GHz. We use herein only the data at the highest available operating frequency $f = 16\,\mathrm{GHz}$. The domain of investigation is a $(15 \times 12)\,\mathrm{cm}^2$ discretized into 50×40 cells.

Figure 7 shows the discretized search domain, the reconstructions obtained with and without regularization after 200 iterations. For this object, a Hebert and Leahy function φ was considered. The results are presented as grey-level map of the normalized non negative imaginary part of the contrast functions. The maximum conductivity is $\sigma = 1.84\,\mathrm{S/m}$ in the non regularized case and $\sigma = 0.31\,\mathrm{S/m}$ in the regularized case.

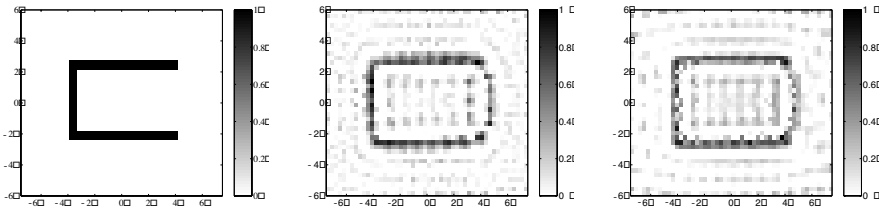

(a) (b) (c)

Figure 7. Reconstructions of the "U-shaped" metallic target at 16 GHz after 200 iterations. Grey scale level of the (a) simulated 15 cm × 12 cm centered search domain discretized into 50 × 40 cells, (b) reconstructed target without regularization and (c) reconstruction obtained using the regularized MGM.

6. CONCLUSION

In this contribution, a regularized modified gradient algorithm was used to solve an inverse scattering problem from laboratory-controlled data. A particular formulation of the MGM was considered in order to efficiently introduce edge-preserving regularization terms which separately act on the real part and on the imaginary part of the contrast function to be estimated. This algorithm was successfully tested against real data, with particularly high-quality estimate of the shape and permittivity level of the dielectric target. As the real data have been determined for different frequencies, future work could be to extend the proposed algorithm to multiple frequencies. Moreover, considering recent work on a multiplicative TV regularization [1], a multiplicative approach would allow one to suppress the empirical choice of the regularization parameter.

REFERENCES

1. Abubakar, A. and P. M. Van Den Berg, "Total variation as a multiplicative constraint for solving inverse problems," *IEEE Trans. on Image Processing,* Vol. 10, No. 9, 1384–1392, 2001.
2. Baussard, A., K. Belkebir, and D. Prémel, "A markovian regularization approach of the modified gradient method for solving a two-dimensional inverse scattering problem," *J. Electromag. Waves and Appl.,* Vol. 17, 989–1008, 2003.
3. Belkebir, K., S. Bonnard, F. Pezin, P. Sabouroux, and M. Saillard, "Validation of 2D inverse scattering algorithms from multi-frequency experimental data," *J. Electromag. Waves and Appl.,* Vol. 14, 1637–1667, 2000.
4. Belkebir, K. and M. Saillard, "Special section: testing inversion algorithms against experimental data," *Inverse Problems,* Vol. 17, 1565–1571, 2001.
5. Blanc-Féraud, L., P. Charbonnier, G. Aubert, and M. Barlaud, "Nonlinear image processing: modeling and fast algorithm for regularization with edge detection," *Proc. IEEE — International Conference on Image Processing (Washington)*, 474–477, 1995.
6. Charbonnier, P., L. Blanc-Féraud, G. Aubert, and M. Barlaud, "Deterministic edge-preserving regularization in computed imaging," *IEEE Trans. on Image Processing,* Vol. 6, No. 2, 298–311, 1997.
7. Delaney, A. H. and Y. Bresler, "Globally convergent edge-preserving regularized reconstruction: an application to limited-

angle tomography," *IEEE Trans. on Image Processing,* Vol. 7, No. 2, 204–221, 1998.

8. Dourthe, C., C. Pichot, J-Y Dauvignac, L. Blanc-Féraud, and M. Barlaud, "Regularized bi-conjugate gradient algorithm for tomographic reconstruction of buried objects," Special issue on problems on random scattering and electromagnetic wave sensing, *IEICE Trans. on Electronics,* Vol. E83-C, No. 12, 1858–1863, 2000.
9. Kleinman, R. E. and P. M. Van Den Berg, "A modified gradient method for two dimensional problems in tomography," *J. Comput. Appl. Math.,* Vol. 42, 17–35, 1992.
10. Lambert, M., D. Lesselier, and B. J. Kooij, "The retrieval of a buried cylindrical obstacle by a constrained modified gradient method in the *h*-polarization case and for Maxwellian materials," *Inverse Problems,* Vol. 14, 1265–1283, 1998.
11. Lobel, P., L. Blanc-Féraud, C. Pichot, and M. Barlaud, "A new regularization scheme for inverse scattering," *Inverse Problems,* Vol. 13, 403–410, 1997.
12. Press, W. H., B. P. Flannery, S. A. Teukolski, and W. T. Vetterling, *Numerical Recipes. The Art of Scientific Computation* Cambridge University Press, Cambridge, 1986.
13. Van Den Berg, P. M. and R. E. Kleinman, "A total variation enhanced modified gradient algorithm for profile reconstruction," *Inverse Problems,* Vol. 11, L5–L10, 1995.

Kamal Belkebir was born in Algeria in 1966. He received the Ph.D. degree in Physics from the University of Paris XI (Orsay), France in 1994. He worked from 1995 to 1997 at the University of Eindhoven, the Netherlands on Post-doctoral position. He joined the Laboratoire d'Optique Electromagnétique in 1997 and he is currently "Maître de Conférences" at the University of Provence in Marseille. His research deals with both forward and inverse scattering techniques.

Alexandre Baussard received the Ph.D. degree in 2003 from "Ecole Normale Supérieure" of Cachan, France. He worked in 2003–2004 at L2S Laboratory within a CNRS post-doctoral position. He is currently "Maître de Conférences" at the "Université de Bretagne Occidentale" working with E3I2 Laboratory. His research deals with inverse problems, multiscale/multiresolution signal and image processing.

Denis Prémel was born in France in 1960. He received the "Agrégation de Génie Electrique" in 1986 and the Ph.D. degree in 1992 from the University of Paris XI (Orsay). He worked from 1994 to 2002 at the Ecole Normale Supérieure de Cachan on a "Maître de Conférences" position. He is currently at the DRT/DETECS/SYSSC/LCME CEA Saclay. His research interests include the development of eddy current simulation tools and inverse scattering methods applied to eddy current non-destructive evaluation.